Anomalous resistivity in a high density FRC

T. P. Intrator*

Los Alamos National Laboratory, M.S. E526, Los Alamos, NM 87545, USA

L. Steinhauer

Redmond Plasma Physics Laboratory, Univ. Washington

R. Renneke, S.C. Hsu, G.A. Wurden, S.Y. Zhang, L. Dorf, W.A. Waganaar

Los Alamos National Laboratory

(Dated: August 2, 2007)

There is a resurgence of interest in high density FRC's as part of a path to fusion relevant plasmas. All theta pinch formed FRCs have some shock heating during formation, but ohmic heating from magnetic flux annihilation is also desirable to heat the ($n > 5x10^{22}m^{-3}$), plasma. At the field null, anomalous resistivity is typically invoked to characterize the resistive like flux dissipation process. The flux dissipation process is both a key issue for MTF and an important underlying physics question We show that the high density FRXL FRC is extremely collisional in the sense that the mean free path for Coulomb collisions can be much smaller than the scale size of this FRC. On the other hand, the Lundquist number is large, and the evaluation of resistivity seems to be amenable to semi empirical scaling laws, which were primarily developed and benchmarked for collisionless Field Reversed Configurations (FRC). We show similarities and differences between the high density FRC data and a database that includes many other FRC experimental data worldwide. The FRXL data extend the known FRC database an order of magnitude or more in density, collisionality, and other dimensionless parameters. Commonly accepted FRC transport and scaling models can then be tested for a wide range of conditions, and then be useful for extrapolation to future plasma compression experiments.

PACS numbers:

I. INTRODUCTION

A compact toroid (Es'kov *et al.* , 1979) (Furth, 1979) (CT) is ideally an axisymmetric magnetic field configuration with currents and magnetic fields that have toroidal symmetry and closed magnetic flux surfaces. One common feature is that these are simply connected geometries, i.e. neither coils, vacuum vessel, nor other objects link the plasma toroid. The CT offers intriguing potential for containing a fusion reactor relevant plasma, due to compact size and efficient confinement of plasma pressure that is nearly equal to the externally applied magnetic field pressure. The taxonomy of CT's encompasses a broad spectrum of possible magnetic configurations including the Field Reversed Configuration (FRC) (Armstrong *et al.* , 1981; Tuszewski, 1988) with magnetic field that is entirely toroidal, the spheromak with equivalent magnitudes of toroidal and poloidal magnetic field (Bussac *et al.* , 1978; Rosenbluth & Bussac, 1979), (Bellan, 2000) the astron (Christofilas, 1959) which has a large ratio of ion gyro radius to plasma dimension, and the field reversed mirror (Pearlstein, 1978) which might be realized as either FRC or spheromak. It has become apparent that at least the FRC and spheromak rely on relaxation processes that involve annihilation of magnetic flux and dissipation of magnetic energy. These processes can include magnetic reconnection and ohmic like dissipation, but are only beginning to be understood.

The FRXL experiment creates a very large density and pressure FRC. Data from FRXL extends the known FRC database an order of magnitude or more in density, collisionality, and other dimensionless parameters. Commonly accepted FRC transport and scaling models can then be tested for a wide range of conditions, and then be useful for extrapolation to future plasma compression experiments.

II. RESISTIVITY

In the context of resistive magnetohydrodynamics (MHD), resistivity η defines a relation between the current density J and the electric field E. A generalized Ohm's Law can include the following terms (and more we omit)

$$\eta J = E + v \times B + \frac{J \times B}{en} - \frac{\nabla p}{en} + ... \qquad (1)$$

where v is the bulk fluid flow, e is electric charge, n is density, and p is a scalar pressure.

Magnetic flux diffusion in space and perpendicular to the local magnetic field lines can be characterized with a

*Electronic address: intrator@lanl.gov

diffusion coefficient

$$D_\eta = \eta_\perp/\mu_0 \tag{2}$$

where we have used the Braginskii estimate for perpendicular and parallel resistivities $\eta_\perp = 1.96\eta_{||}$. Flux dissipation can be accounted for by a dissipated power density $\mathcal{P} = \eta J^2$. Resistivity can be written in terms of a collision frequency ν

$$\eta = \frac{\nu}{\omega_{pe}^2 \epsilon_0} \tag{3}$$

where ω_{pe} is the electron plasma frequency. One might expect ν to correspond to the coulomb collision scattering for charged particle collisions $\nu = \nu_C$ However in many interesting plasmas, including experiments (**?**) space, astro and solar physics plasmas, the coulomb collisionality is far less than would be required to explain the inferred large apparent resistivities. In this sense these plasmas can be regarded as *collisionless* which exhibit a resistivity η^* that is *anomalously* large.

Recently, experiments have demonstrated that it is possible to vary the Coulomb collisionality over a wide range, and estimate the apparent anomalousness of the resistivity (Trintchouk *et al.* , 2003) (Intrator *et al.* , 2004). The microphysics origin of the anomalous collisionality has been the subject of extensive speculation over the last 50 years. In the MRX magnetic reconnection experiment, an electromagnetic branch of the Lower Hybrid Drift instability (LHDI) has been implicated but it is not known if this a general conclusion for any other examples in nature or laboratory. (Kulsrud *et al.* , 2005) (Ji *et al.* , 2005). Other estimates of η^* for FRC's have shown an anomalous factor $\eta^*/\eta_\perp$ of 1-20 for a wide range of FRC parameters (Tuszewski, 1988) and for spheromaks (Bellan, 2000). The Lundquist number is a useful figure of merit that compares the collisionality is the ratio of resistive diffusion time τ_R to Alfven transit time τ_A .

$$S = \frac{\tau_R}{\tau_A} = \frac{L v_A}{\eta_\perp/\mu_0} \tag{4}$$

where L is the length scale of interest, v_A is the Alfven speed, and $\tau_A = L/v_A$.

III. FRC EXPERIMENT WITH A WIDE RANGE OF COLLISIONALITY

It would be useful if one could separately vary the Coulomb collisionality and the Lundquist number. The FRX-L experiment at LANL is a small, high density experiment that relies on a moderate energy but high voltage main capacitor bank and small size to operate with a large toroidal electric field. FRX-L (Taccetti *et al.* , 2002) (Intrator *et al.* , 2004) (Zhang *et al.* , 2005) is a high density FRC intended to create a robust plasma target for Magnetized Target Fusion (**?**) (Intrator *et al.* , 2004) (Kirkpatrick *et al.* , 1995). that has both a large range of experimentally accessible density and electron temperature T_e so that a wide range of coulomb collisionalities can be experimentally accessed.

The FRC parameter space including high density was only briefly explored in the early days of fusion research, which focused on the theta pinch. In the 1960's and 1970's it was shown that (Eberhagen & Grossmann, 1971) (McLean *et al.* , 1967) (Kaleck *et al.* , 1967) high density theta pinches and FRC's were possible. But subsequent interest in tokamaks diverted interest from these concepts. Today with more sophisticated diagnostics and appreciation for CT's, we are attempting to improve the physics understanding of these plasmas, rediscover how they were formed, and improve upon them for applications that include MTF.

For the FRC data we show here, we will refer to a cylindrical (r, θ, z) geometry as shown in figure 1. The axis of symmetry is $\hat{z}$, the toroidal direction is $\hat{\theta}$, and $\hat{r}$ is radial. The radial location of the magnetic null is at $r = R = r_s/\sqrt{2}$, the separatrix radius is r_s. A single turn theta coil forms a flux conserving boundary at inner radius at $r = r_c$.

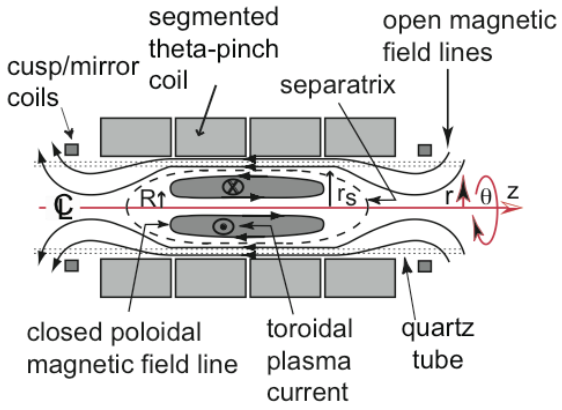

FIG. 1 Geometry of a typical FRC

Time history data from a representative shot is shown in figure 2, where the plasma pressure $p = nT$ is shown in figure 2(a), chord averaged density in figure 2(b), chord averaged total temperature $T = T_e + T_i$ in figure 2(c), volume averaged beta in figure 2(d), local magnetic field at the midplane in figure 2(e), and separatrix radius at the midplane in figure 2(f). These data were obtained with a static D2 prefill of $p_0 = 50mT$. Figure 2 shows a typical recent shot, with large plasma pressure of $nk_BT \approx 2 - 3MPa$ compared to other fusion devices.

The Coulomb mean free path for electron scattering off of ions λ_{ei} is approximately equal to the ion-ion scattering mean free path λ_{ii}. If the FRX-L plasma is to be collisional, the plasma size which we deem to be the separatrix radius must be large $r_s/\lambda_{ii} >> 1$ compared to the scattering length. A survey of many (i.e. 85) shots for a

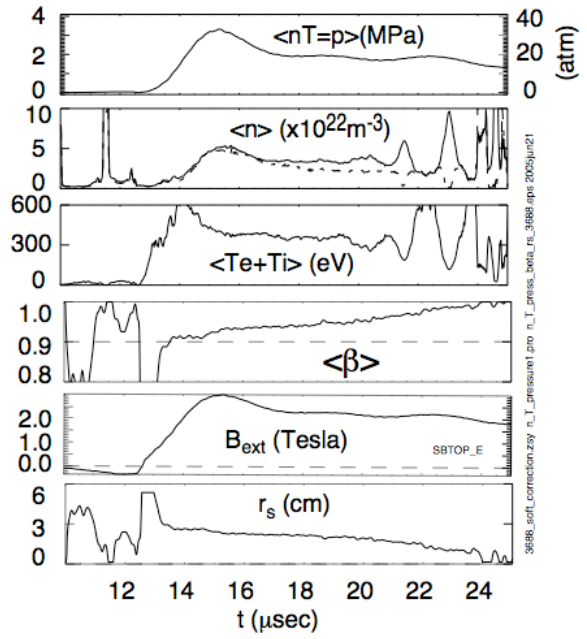

FIG. 2 shot 3688

variety of gas prefill levels, main bank voltage was taken. A comparison is possible among many FRC experiments for different geometry.

The path to interesting fusion relevant parameters many CT plasma devices including FRC's is likely to lead to large densities. On the other hand most of the existing FRC database has been developed for experiments at substantially smaller densities than FRXL. We would like to test the extrapolation of existing scaling laws and physics understanding to much higher density regimes, and see whether new physics enters into play.

The flux confinement time is one measure of the magnetic confinement of the FRC configuration. Magnetic flux is thought to be dissipated at the O-point, and its decay is usually parameterized using a resistivity and diffusivity as in equation 2. The flux confinement time is traditionally scaled against a parameter that is a useful yardstick R^2/ρ_{ie} (Tuszewski, 1988), where ρ_{ie} is the ion gyro radius referenced to the external magnetic field. This parameter can be used to compare different experiments with different sizes and other plasma parameters. The relationship is usually taken to be

$$\tau_\phi[\mu sec] \approx a_\phi \frac{R[cm]^2}{\rho_{ie}[cm]} \tag{5}$$

where the coefficient $a_\phi \approx 0.5$. We plot the FRC database and the higher density FRXL data against this parameter. This seems to fit the world FRC database approximately. On the other hand, the although the slope corresponding the FRXL data is indicates a stronger dependence than linear on this fit parameter

$$\tau_\phi[\mu sec] \approx a_{\phi,FRXL} \left(\frac{R[cm]^2}{\rho_{ie}[cm]} \right)^{b_\phi} \tag{6}$$

where the coefficient $b_\phi \approx 2$.

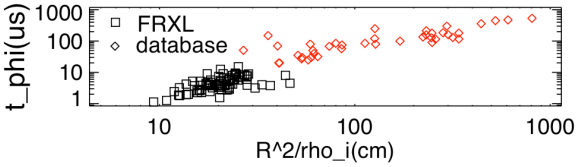

FIG. 3 Plot of flux confinement time vs the usual scaling parameter R^2/ρ_i. The scaling is approximately linear for the lower density FRC's and worse for high density FRC's.

IV. RESISTIVITY

Theta pinch formed FRC's are initially heated during formation by a shock, but later during the decay phase substantial ohmic heating is expected to sustain the plasma temperature. This could be increased by anomalously enhanced resistivity

$$\eta^* = \nu^*/(\omega_{pe}^2 \epsilon_0) \tag{7}$$

over the Spitzer value

$$\eta_\perp \approx 2\eta_{||} = \nu_{ei}/(\omega_{pe}^2 \epsilon_0) \tag{8}$$

where ν^* (ν_{ei}) is the anomalous (electron-ion) collision frequency and ω_{pe} is the electron plasma frequency. The anomaly factor for FRC's has traditionally been reported to be in the range of $\eta^*/\eta_\perp \approx 2 - 20$ (Tuszewski, 1988).

The resistivity at the magnetic null can be evaluated for a rigid rotor type profile model. In the spirit of equation 2

$$\frac{\eta^*(R)}{\mu_0} = \frac{R^2}{4\tau_\phi} \frac{\ln[cosh(k)]}{k^2} \tag{9}$$

we experimentally determine r_s, and τ_ϕ, assume $R = r_s/\sqrt{2}$ and use these to infer η^*. The parameter k is a rigid rotor shape factor where the model $B_{pol}(r) = tanh[k(r^2/R^2 - 1)]$.

A survey of the normalized resistivities for a wide range of FRC experiments is displayed in figure 4

FRXL anomaly factor $\eta^*/\eta_\perp$ data show substantial scatter, decreasing to small $\eta^*/\eta_\perp$ with Coulomb collisionality for $r_s/\lambda_{ei} > 10$ in Fig. 4(a) and increasing with Lundquist number $S = r_s v_A/(\eta_\perp/\mu_0) \gg 1$ in Fig. 4(b). For a range of densities and total temperature $T_{tot} = T_e + T_i$, we have assumed $T_e \approx T_{tot}/2$, and $T_e(T_i)$ are respectively the electron and ion temperatures. We note that MRX (Trintchouk *et al.* , 2003) reconnection

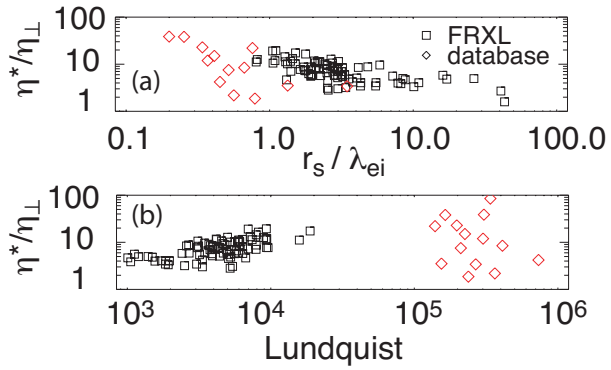

FIG. 4 Comparison of inferred anomalous resistivity normalized to the perpendicular Spitzer resistivity as a function of (a) the coulomb collisionality figure of merit r_s/λ_{ii} and (b) the Lundquist number as shown on the horizontal axis.

experiments showed $\eta^*/\eta_\perp > 5-10$ for $\delta/\lambda_{ei} > 1$, where δ was a reconnection layer width.

When the FRC is much larger than the Coulomb collision mean free path, the anomalous factor gradually decreases to a factor of 1 to 2. For the FRX data the resistivity anomaly increases with Lundquist number. Figure 4(b) shows that for the rest of the world FRC database, there is a lot of scatter in the data.

V. MODELS FOR ANOMALOUS COLLISIONALITY

A. Phenomological model

One can compare the anomalous collision frequency ν^* to a phenomenological reference collision frequency (Milroy & Brackbill, 1986)

$$\nu^*_{ph} = C_{ph}\omega_{pi}\left(\frac{v_{eD}}{v_i}\right)^2 \tag{10}$$

for a wide range of FRC data. This comparison is shown in figure 5 When this quantity is plotted against the collisionality figure of merit, there is not much correlation for

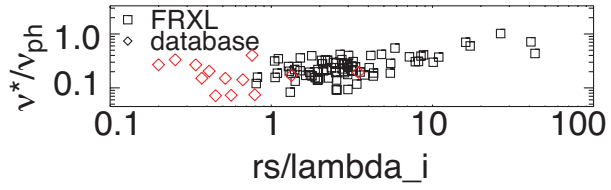

FIG. 5 Comparison of inferred anomalous collision frequency with a phenomenological collision frequency that scales with the ion plasma frequency and an electron drift parameter. The data from the world FRC database (diamonds) and FRXL (squares) span a large range in coulomb collisionality figure of merit r_s/λ_{ii} shown on the horizontal axis.

the world FRC data base. But for the highly collisional FRXL data, there is a discernible trend. At the highest collisionality, $\nu^*/\nu^*_{ph} \approx 1$ for $r_s/\lambda_{ii} >> 1$.

$$\eta^* = \nu^*/(\omega^2_{pe}\epsilon_0) \tag{11}$$

over the Spitzer value

$$\eta_\perp \approx 2\eta_{||} = \nu_{ei}/(\omega^2_{pe}\epsilon_0) \tag{12}$$

The anomalous physics has never been explained, but ν^* is typically attributed to particle scattering from a wave energy density proportional to the internal poloidal magnetic field energy density. Here we calculate the resistivity using a rigid rotor model (Hoffman *et al.* , 1982) that was benchmarked on FRXL using a multi chord interferometer (Intrator *et al.* , 2004).

Errors in the drift correction to the anomalous collision frequency from equation 10 may be substantial, since one must estimate the current density and infer the electron drift speed. Figure 6 shows a plot of ν^* dependence on the ion plasma frequency and a significant correlation.

B. Two point transport model

Consideration of the 2PT requires separate measurements of the particle τ_N and flux $\tau\phi$ confinement times. FRX-L is one of the few experiments that has measured them both, so that a comparison with the global FRC database does not have that many data points besides FRXL at high density.

Also indicated are the calculated anomalous collision frequencies based on the *Two Point Transport* model (2PT) that assumes self similar decay of the FRC and its gradients in magnetic field and particle density. 2PT predicts enhanced $\nu^*(r_s)$ and reduced $\nu^*(R_0)$. For these data the $\nu^*(r_s)$ follows from a particle confinement time and edge gradient length $L_n \approx 2\rho_{ie}$ where ρ_{ie} is the ion gyro radius referenced to the external magnetic field B_e. At the O-point, $\nu^*(R_0)$ is inferred in the usual way from flux confinement time, but constrained so that the flux and density gradients are consistent with self similar decay.

C. Wave energy bound model

If the resistivity is due to particle scattering off waves, then a force density that could account for the scattering may be written in terms of a gradient of some energy density

$$eEn = \eta^* Jen \tag{13}$$
$$\eta^* Jen = -\nabla_\perp W(r) \tag{14}$$

Invoking equation 11 the collision frequency can be written in terms of B_{pol}

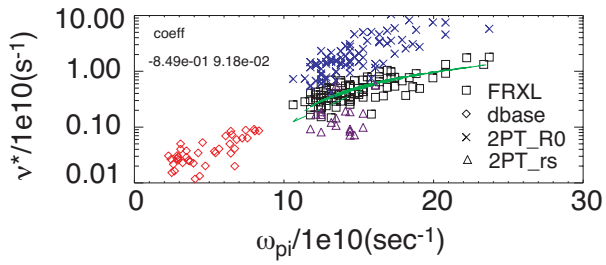

FIG. 6 FRXL shot data (squares) and a survey of many other lower density FRC experiments (diamonds, courtesy L. Steinhauer) comparing anomalous collision frequency ν^* with ion plasma frequency. Also shown are the 2PT predictions for $\nu^*_{2PT}(r_s)$ (triangles) and $\nu^*_{2PT}(R_0)(x's)$.

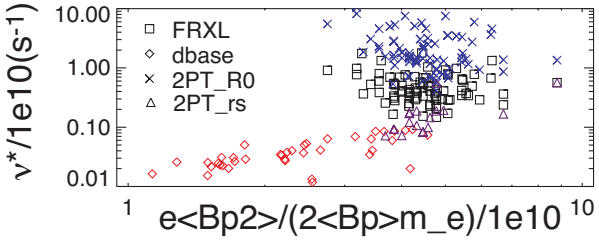

FIG. 7 FRXL shot data (squares) and a survey of many other lower density FRC experiments (diamonds, courtesy L. Steinhauer) comparing anomalous resistivity η^* with a wave scattering electric force proportional to a gradient of internal poloidal magnetic field energy. Also shown are the 2PT predictions for $\nu^*_{2PT}(r_s)$ (triangles) and $\nu^*_{2PT}(R_0)(x's)$.

$$\nu^* = -\frac{e\mu_0}{m_e}\frac{\nabla_\perp W(r)}{\nabla \times B_{pol}} \tag{15}$$

The scattering could be from waves driven by magnetic energy density where

$$W_B(r) = \frac{B^2_{pol}(r)}{2\mu_0} \tag{16}$$

or particle pressure where

$$W_p(r) = p(r) = n(r)T(r) \tag{17}$$

For the magnetic energy density W_B the perpendicular gradient can be approximated as

$$\nabla_\perp W(r) = \frac{B^2_{pol}(r)}{2\mu_0(r_s - R)} \tag{18}$$

$$\approx \frac{B^2_{ext}(r)}{2\mu_0(r_s - R)} \tag{19}$$

Equation 19 can be estimated by evaluating a volume averaged $< B^2_{pol} >$, which follows from the Barnes relation $< \beta >= 1 - x_s^2/2$ where $x_s = r_s/r_c$ is the separatrix radius $r_s = \sqrt{2}R_0$ normalized to the coil radius r_c, and the magnetic null radius is R_0.

$$\frac{< B^2_{pol} >^2}{B_{ext}} = \left(\frac{R_0}{r_c}\right)^2 \tag{20}$$

The volume averaged poloidal field we define using the poloidal flux $\phi_{pol} = \pi R_0^2 < B_{pol} >$ is approximated using the scaling relations (Tuszewski, 1988)

$$\phi_{pol} = \pi r_c^2 B_{ext}\left(\frac{R_0}{r_c}\right)^{3+\epsilon} \tag{21}$$

$$< B_{pol} > = B_{ext}\left(\frac{R_0}{r_c}\right)^{1+\epsilon} \tag{22}$$

Here $\epsilon \approx 0.25$ is an edge shape factor. At the crude level of this estimate, the differential operators for equations 15 can be approximated using the FRC scale length $r_s - R_0 = (\sqrt{2} - 1)R_0$. Therefore the volume averaged anomalous collision frequency should scale as an electron gyro frequency with effective magnetic field $< B^2_{pol} > / < B_{pol} >$

$$< \nu^* >= \frac{e}{2m_e}\frac{< B^2_{pol} >}{< B_{pol} >} \tag{23}$$

Figure 7 data indicates reduced scatter when plotted against a wave scattering ν^* proportional to internal poloidal magnetic field B_{pol} energy W. This is reminiscent of lower hybrid drift wave scaling (Milroy & Brackbill, 1982) (Tuszewski, 1988) and more general than the result shown by (Winske & Liewer, 1978) and requires that $\eta^* \approx C_{wave}B_{ext}x_s^{1+\epsilon}/n$, $\epsilon \approx 0.25$ is an edge shape factor, and n is average density. Error bars for $\eta^*/\eta_\perp$ may be sensitive to impurities(Tuszewski, 1988) $Z_{eff} \leq 1.5$, FRC profile deviation from the rigid rotor model, and whether $T_e \approx T_{tot}/2$. High density plasmas are expected to exhibit low Z_{eff} (Matthews *et al.* , 1997).

Also shown are the 2PT predictions for $\nu^*_{2PT}(r_s)$ (triangles) and $\nu^*_{2PT}(R_0)(x's)$. The inferred values for separatrix $\nu^*_{2PT}(r_s)$ are consistent with the wave energy bound model described above.

D. Does FRC reconnection resemble Sweet-Parker?

We believe that magnetic flux annihilation that is part of a magnetic reconnection process at the O-point drives ohmic heating of the plasma. The prevalent model invokes a modified Sweet-Parker model with fluid inflow driven by $v_{in} = E \times B/B^2$ drift. The E is is the reconnection electric field and the B is the reconnecting magnetic field that has oppositely directed components in the reconnection region. The Alfven Mach number $M_A = v_{in}/v_A$ is proportional to the presumed reconnection rate, where v_A is the Alfven speed referenced to the asymptotic magnetic field outside the reconnection region and is analogous to B_e in the FRC case.

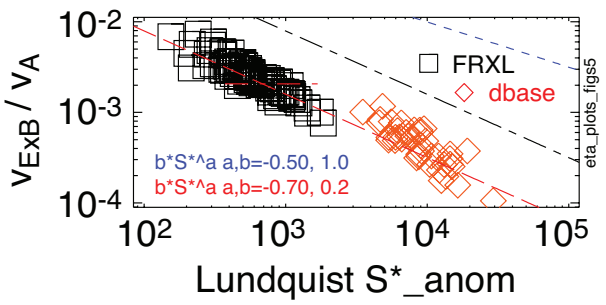

FIG. 8 FRXL shot data showing the inferred normalized reconnection rate as the ratio of the inflow short dash line corresponds to $S*^{-1/2}$ and the red long dash line corresponds to $0.2S*^{-0.7}$.

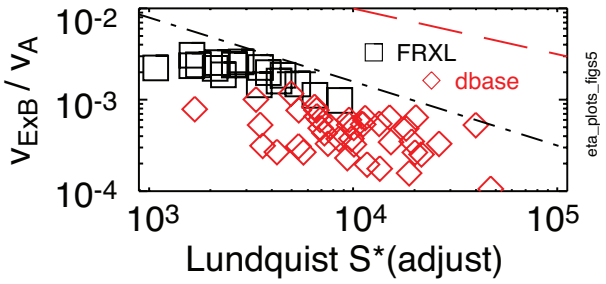

FIG. 9 FRXL shot data showing the inferred inflow Mach number plotted against the modified Lundquist number S^* including compessibility and finite downstream pressure. The red dashed line corresponds to $S*^{-1/2}$ and the dash-dot line corresponds to $S*^{-0.7}$.

The usual picture of reconnection requires an anomalously large Lundquist number S^* that follows from anomalously large resistivity. In the MRX experiment (Trintchouk *et al.* , 2003) , (Ji *et al.* , 1998), the reconnection rate was shown fit this model and to be proportional to the inverse square root of the anomalous Lundquist number $M_A \approx 0.2S*^{-0.7} \propto 1/S^{*1/2}$. The predicted $S*^{-1/2}$ dependence results in a fit that is two orders of magnitude too large. Nevertheless, there is some evidence in figure 8 that FRX-L data does fit some model where Lundquist number collapses much of the data to a line.

Another plot 9 invokes a modified Lundquist number that includes compressibility and finite downstream pressure. The modified $S*^{-0.7}$ slope seems to represent an upper bound for the data, but with substantially more scatter than when the same plot is referenced to the unmodified $S*$.

VI. DISCUSSION

There is a resurgence of interest in high density FRC's as part of a path to fusion relevant plasmas. All theta pinch formed FRCs have some shock heating during formation, but ohmic heating from magnetic flux annihilation is also desirable to heat the ($n > 5x10^{22}m^{-3}$), plasma. At the field null, anomalous resistivity is typically invoked to characterize the resistive like flux dissipation process.

The flux dissipation process is both a key issue for MTF and an important underlying physics question We show that the high density FRXL FRC is extremely collisional in the sense that the mean free path for Coulomb collisions is much smaller than the scale size of this FRC. On the other hand, the Lundquist number is large, and the evaluation of resistivity seems to be amenable to semi empirical scaling laws, which were primarily developed and benchmarked for collisionless Field Reversed Configurations (FRC).

We show similarities and differences between the high density FRC data and a database that includes many other FRC experimental data worldwide. It is useful that the range of Lundquist number S that is available for theoretical modeling now spans 4 decades, and the anomalous Lundquist number S now spans 3 decades. This can help constrain theoretical models and significantly expands the existing experimental data base both for FRC's and other laboratory experiments. These data may be useful for extrapolation from existing FRC's to future plasma compression experiments.

Acknowledgments

This work was supported by Los Alamos National Laboratory, U.S. Department of Energy under Contract No. W-7405-ENG-36.

References

Armstrong, W. T., Linford, R. K., Lipson, J., Platts, D. A., Sherwood, & E, G. 1981. Field-reversed experiments on compact toroids. *Physics of Fluids*, **24**.

Bellan, P. M. 2000. *Spheromaks: A practical application of magnetohydrodynamic dynamos and plasma self organization.* 57 Shelton St., Covent Garden, London UK: Imperial College Press.

Bussac, MN, Furth, HP, Okabayashi, M, Rosenbluth, MN, & Todd, AM. 1978. *Plasma Physics and Controlled Nuclear Fusion Research, IAEA, Vienna*, **II**.

Christofilas, NC. 1959. *Progress in Nuclear Energy; Series XI - Plasma Physics and Controlled Nuclear Fusion*, **1**.

Eberhagen, A., & Grossmann, W. 1971. Theta pinch experiments with trapped antiparallel magnetic fields. *Zeitschrift fur Phys.*, **248**.

Es'kov, A. G., Kurtmullaev, R. K., Kreshchuk, A. P., Laukhin, Y. N., Malyutin, A. I., Markin, A. I., Martyushov, Y. S., Mironov, B. N., Orlov, M. M., Proshletsov, A. P., Semenov, V. N., & Sosunov, Y. B. 1979. Principles of plasma heating and confinement in a compact toroidal configuration. *Nuclear Fusion*, **2**.

Furth, HP. 1979. Compact Toruses and Energetic Particle Injection. Proc. Us-Japan Joint Symposium, Princeton N.J. USA: Princeton Plasma Physics Laboratory.

Hoffman, A. L., Milroy, R. D., & Steinhauer, L. C. 1982. Poloidal flux loss in a field reversed theta pinch. *Applied Phys Lett*, **41**.

Intrator, T., Zhang, S. Y., Degnan, J. H., Furno, I., Grabowski, C., Hsu, S. C., Ruden, E. L., Sanchez, P. G., Taccetti, J. M., & Tuszewski, M. 2004. A high density field reversed configuration (FRC) target for magnetized target fusion: first internal profile measurements of a high density FRC. *Physics of Plasmas*, **11**(5).

Ji, H., Yamada, M., Hsu, S., & Kulsrud, R. 1998. Experimental Test of the Sweet-Parker Model of Magnetic Reconnection. *Physical Review Letters*, **80**(15).

Ji, H. T., Kulsrud, R., Fox, W., & Yamada, M. 2005. An obliquely propagating electromagnetic drift instability in the lower hybrid frequency range. *Journal of Geophysical Research-Space Physics*, **110**(A8).

Kaleck, A., Kever, H., Konen, L., Noll, P., Sugita, K., Waelbroeck, F., & Witulski, H. 1967. Study of trapped reverse field configurations in a linear thetapinch experiment. vol. LA-3770. Los Alamos Scientific Laboratory.

Kirkpatrick, R. C., Lindemuth, I. R., & Ward, M. S. 1995. Magnetized target fusion - an overview. *Fusion Technology*, **27**.

Kulsrud, Russell, Ji, Hantao, Fox, William, & Yamada, Masaaki. 2005. An electromagnetic darift instability in the magnetic reconnection experiment and its importance for magnetic reconnection. *Physics of Plasmas*, **12**(8).

Matthews, G. F., Allen, S., Asakura, N., Goetz, J., Guo, H., Kallenbach, A., Lipschultz, B., McCormick, K., Stamp, M., Samm, U., Stangeby, P. C., Steuer, K. H., Taroni, A., Unterberg, B., & West, P. 1997. Scaling radiative plasmas to ITER. *Journal of Nuclear Materials*, **241-243**.

McLean, E. A., Anderson, A. D., & Griem, H. R. 1967. Measurement of plasma density and particle losses in a large theta pinch. vol. LA-3770. Los Alamos Scientific Laboratory.

Milroy, R. D., & Brackbill, J. U. 1982. Numerical studies of a field-reversed theta-pinch plasma. *Phys. Fluids*, **25**.

Milroy, R. D., & Brackbill, J. U. 1986. Toroidal magnetic field generation during compact toroid formation in a field-reversed theta pinch and a conical theta pinch. *Physics of Fluids*, **29**(4).

Pearlstein, L. D. 1978. *Plasma Physics and Controlled Nuclear Fusion Research, IAEA, Vienna*, **II**.

Rosenbluth, MN, & Bussac, MN. 1979. *Nucl. Fusion*, **19**.

Taccetti, J. M., Intrator, T. P., Wysocki, F. J., Forman, K. C., Gale, D. G., Coffey, S. K., Degnan, & J, H. 2002. Magnetic field measurements inside a converging flux conserver for magnetized target fusion applications. *Fusion Sci. Tech.*

Trintchouk, F., Yamada, M., Ji, H., Kulsrud, R. M., & Carter, T. A. 2003. Measurement of the transverse Spitzer resistivity during collisional magnetic reconnection. *Physics of Plasmas*, **10**(1).

Tuszewski, M. 1988. Field Reversed Configurations. *Nucl. Fusion*, **28**.

Winske, D., & Liewer, P. C. 1978. Particle simulation studies of the lower hybrid drift instability. *Physics of Fluids*, **21**(6).

Zhang, S., Intrator, T. P., Wurden, G. A., Waganaar, W. J., Taccetti, J. M., Renneke, R., Grabowski, C., & Ruden, E. L. 2005. Confinement analyses of the high-density field-reversed configuration plasma in the field-reversed configuration experiment with a liner. *Physics of Plasmas*, **12**(5).